JJEE
Volume 12 | Number 2 | June 2026 | Pages 209-224

Jordan Journal of Electrical Engineering

ISSN (print): 2409-9600, ISSN (online): 2409-9619

Homepage: jjee.ttu.edu.jo

Solar-Powered Seawater Reverse Osmosis Desalination in Jubail: A Comparative Techno-Economic Analysis of PV and CSP Using SAM

Muetaz Mohammed

Department of Mechanical Engineering, King Fahd University of Petroleum & Minerals, Dhahran, Saudi Arabia
E-mail: g202419800@kfupm.edu.sa

Received: Jan 24, 2026 *Revised: Feb 25, 2026* *Accepted: Apr 22, 2026* *Available online: Jun 15, 2026*

***Abstract*—** This paper offers a techno-economic benchmarking of solar electricity alternatives for driving seawater reverse osmosis (SWRO) desalination in Jubail, Saudi Arabia, using the System Advisor Model (SAM) from NREL. The alternatives include photovoltaics (PV) and three concentrated solar power (CSP) alternatives: linear Fresnel (LF), parabolic trough (PT), and solar tower (ST). The SWRO electricity demand is specified as 160 GWh/year with a specific energy consumption of 3.5 kWh/m3, and the analysis is carried out in a grid-connected annual offset mode to ensure continuous plant operation. The economic analysis is carried out over a 25-year project life with a real discount rate of 5.5% and a water tariff of 2.14 USD/m3. The calculated levelized cost of water (LCOW) clearly shows that PV has the lowest LCOW 0.82 USD/m3, followed by PT 1.44 USD/m3, ST 1.52 USD/m3, and LF 1.77 USD/m3. While PV has the lowest LCOW, the NPV analysis shows that all alternatives have positive project viability with NPVs of 0.96, 13.21, 17.61, and 18.95 million USD for PV, PT, ST, and LF, respectively. In summary, the analysis clearly shows that technology differences under identical site conditions lead to significantly different desalination costs and investment indicators.

***Keywords*—** Techno-economic analysis; PV system; CSP systems; Reverse osmosis; System advisor model.

1. INTRODUCTION

Energy and water are essential for preserving an ecosystem and environment that support all living forms. They are essential to the fulfillment of social and economic development as well as the fundamental human necessities of life and health [1]. Water makes up about 326 million cubic miles, or 71% of the earth's surface. The oceans contain 97.5% of the water on Earth, which is too salty for drinking, growing crops, and most industrial uses other than cooling (Fig. 1). Only 2.5% of the water on Earth is fresh. However, only about 0.5% is readily accessible freshwater, and the remaining 2.0% is unreachable due to its presence in glaciers, polar ice caps, the atmosphere, highly contaminated soil, and deep underground areas that are expensive to access [2, 3].

Access to clean water is a critical component of basic human functions such as drinking, household use, agriculture, and industry [4]. A minimum estimate of basic requirements would be around 1000 m^3 per capita per year [12]. Falkenmark's scale suggests that water stress is generally considered to be below 1000-1700 m^3 per capita per year, while water scarcity is below 1000 m^3 per capita per year [5]. In line with these estimates, freshwater scarcity has emerged as a rising global problem, with an estimated 3.7×10^9 people suffering from water scarcity, which could rise by 2×10^9 by 2050 [6, 7].

* Corresponding author
DOI: https://doi.org/10.5455/jjee.204-1769285037

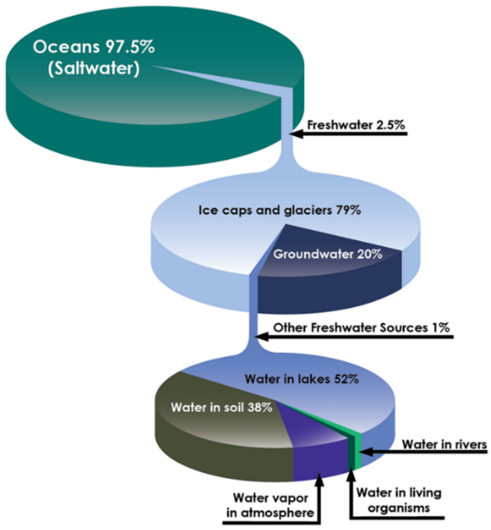

Fig. 1. Freshwater distribution in the earth.

According to the Food and Agriculture Organization (FAO) of the United Nations, 1.2×10^9 people, mostly living in arid or semi-arid areas, are affected by physical water scarcity [8]. Moreover, the increasing demand for access to clean water could pose severe socio-economic and environmental constraints if supply-side measures are not increased correspondingly. Looking ahead, the Population Action International Institute forecasts that by 2050, the global distribution of population with respect to relative sufficiency, water stress, and scarcity will be 58%, 24%, and 18%, respectively [9]. Fig. 2 illustrates the global distribution of water stress and points out that Saudi Arabia is categorized under the very high water stress group; this categorization is in line with the country's mostly arid climate and low renewable freshwater resources [10].

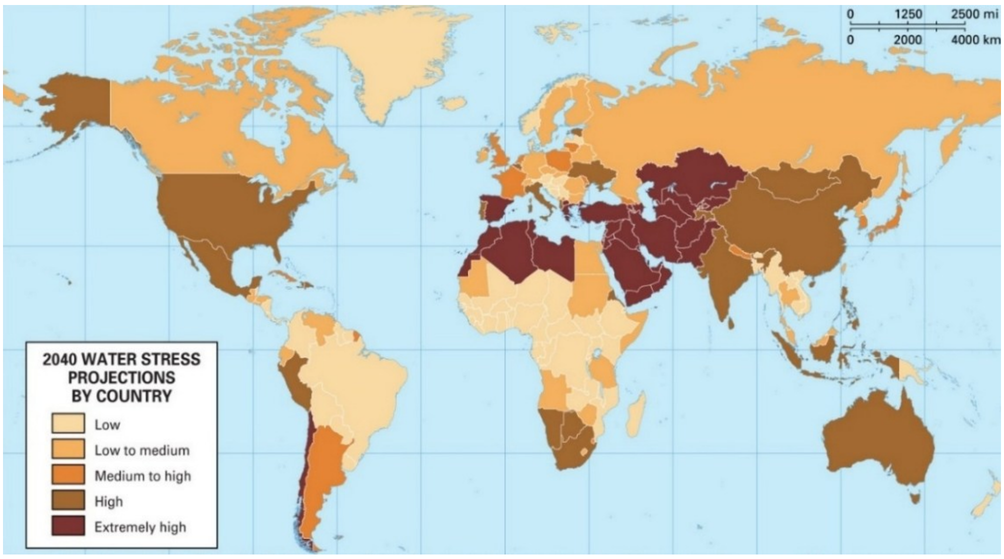

Fig. 2. Worldwide water stress [9].

However, beyond physical scarcity indicators, equitable access to safely managed drinking water remains a major global challenge. The UNICEF estimates that 884×10^6 people drink tainted water. Boreholes, household connections, protected springs, rainwater, public standpipes, and protected dug wells are among the approximately 60% of people that use improved potable water for drinking [11]. The usage of clean water in 2023 is shown in Fig. 3.

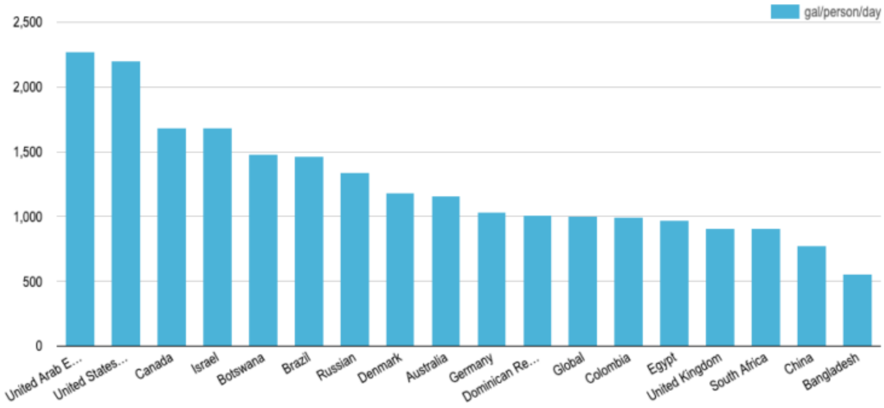

Fig. 3. Worldwide usage of potable water in 2023 [11].

These trends collectively indicate a widening gap between freshwater availability and demand, especially in arid and semi-arid regions. Consequently, non-conventional water supply options are increasingly required, among which desalination has become a key solution for producing potable water at scale. Desalination is a key solution for meeting freshwater demand in arid regions to address water scarcity. According to the source, desalination is a method of water purification that eliminates all dissolved salts and minerals from saltwater to produce drinking water [12]. Based on [13], there are two different types of total dissolved solids (TDS) in saline water: brackish water, where TDS levels can reach 10×10^3 ppm, and saltwater, where TDS levels can reach 45×10^3 ppm. According to the source [14], the acceptable range for salt concentration in drinking water is between 500 and 1,000 parts per million. Fig. *4* lists the two primary desalination techniques, thermal desalination and membrane desalination.

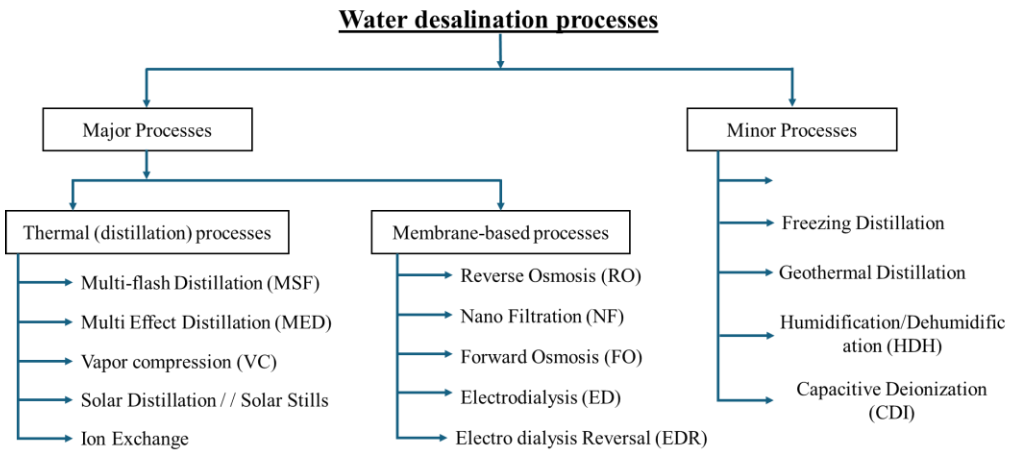

Fig. 4. Desalination process types [14].

The thermal type which applies heat to separate salt from water, relies on two successive stages of vaporizing the saline water and then condensing the distillate vapor to eliminate salt from saline water. Offers a major capacity for fresh water and can be grouped into multi-stage flash (MSF), multi-effect evaporation (MEE) or Multi-effect desalination (MED), and thermal or mechanical vapor compression [12].

In the case of MSF desalination, water is produced by successive processes of evaporation and condensation. The process of flashing takes place when the heated saline water is subjected to chambers that have lower pressures. This results in the production of vapor without the need for the water to boil. The produced vapor is then subjected to the condensation process, and the heat of condensation is normally utilized to heat the water as it enters the system. The MSF method is one of the most used methods in the production of desalinated water, contributing a significant amount to the global capacity of desalination plants [15].

The MEE resembles MSF in being a thermal, staged desalination process; however, it differs in how heat is recovered and reused. In MEE, the vapor produced in one effect condenses in the next, and the released latent heat is used to evaporate additional feedwater, which can enhance overall efficiency. System performance is typically improved by operating successive effects at progressively lower pressures. Despite its high potential performance, large-scale adoption of MEE has often been constrained by tube scaling. MEE also offers flexibility in selecting high- or low-temperature operating designs, which may help reduce corrosion and fouling tendencies, although scaling can still remain significant. In contrast to MSF where evaporation mainly occurs due to flashing after a pressure drop MEE involves boiling/evaporation at heat-transfer surfaces, which increases the likelihood of scale formation; nevertheless, reduced tube-surface scaling has been reported under appropriate conditions [16].

In terms of industrial desalination, membrane techniques are also crucial technology. These techniques fall into two categories: electric dialysis (ED) and reverse osmosis (RO). In order for the solute on one side and the solvent on the other to pass through the membrane, reverse osmosis increases as the saline water pressure rises. RO is mostly used for large-scale plants, ED operations use electricity and a particular ion-exchange membrane, and both RO and ED can be used with low salinity. Both technologies can be used with low salinity, however RO is primarily used for large-scale plants [17].

In a typical RO plant, 3-5 kWh of electricity and 0.5-2.5 kWh of brackish water are needed to produce 1 m^3 of freshwater from seawater. In fact, around eighty percent of desalination facilities today use RO as their separation method, according to the International Desalination Association's most recent study. Because it uses less energy, uses less water, and has higher water recovery factors than any conventional method, this technology is successful [18].

However, desalination consumes a lot of energy; each year, about 10 kilotons of fossil fuel are required to produce 1,000 m^3 of water per day [19]. It is now essential to replace the depleted fossil fuel with sustainable and renewable energy sources in order to lower the carbon footprint and greenhouse gas (GHG) emissions, which are the main causes of global warming and climate change [20].

The RO plant requires energy, which is its vital operational resource. Desalination plant requires continuous operation powered by renewable energy sources that offer limitless energy [21]. Solar energy is one of the most viable options for saltwater desalination due to its limitless energy production with no environmental impacts, being a renewable energy source. Solar energy is used as an energy source that powers the world's energy system due to its widespread use of photovoltaic technology [22].

In contrast to direct methods, indirect solar desalination collects and transfers heat from solar radiation to evaporate saline water. In order to reduce the loss of latent heat from condensation, the other type is seen as a distinct system consisting of a variety of solar heating devices, such as thermal or photovoltaic collectors, and a traditional desalination unit. While some methods can be used with PV technology, such as ED and RO, solar desalination units that rely on both vaporizing and condensing principles use evacuated tubes, flat-plate collectors, or solar concentrators like MSF, MED, TVC, and MD. When wind energy is available because electricity is required, ED and RO are used [12].

Though solar-based desalination receives considerable attention, general technology-to-technology comparisons are difficult to find due to the non-uniform nature of assumptions, geographical points, and load definitions in most studies, which makes it difficult to compare them on an equal footing. To fill this research gap, the originality of this research effort is to provide a same-site and same-load techno-economic comparison of PV and CSP technologies, including linear Fresnel (LF), parabolic trough (PT), and solar tower (ST) systems for driving SWRO-based desalination in Jubail, Saudi Arabia, in a single modeling framework. The originality of this research effort lies in establishing a connection between the irradiance/DNI pattern and the differences in monthly energy production, which are then used to derive investment-related metrics (LCOW, NPV, and lifespan revenue) to provide a meaningful comparison. Future research efforts should focus on incorporating storage-based dispatch optimization, sensitivity/uncertainty analysis, and multi-location comparisons to improve the generality of the results, which are currently based on current limitations (no storage and simplified operation).

2. METHODOLOGY

The methodological framework used in this study (Fig. 5) combines solar assessment, SAM simulation, SWRO electricity demand integration, and techno-economic evaluation in a unique comparative framework. The analysis process follows three sequential steps: (i) the simulation of the technical performance of the PV and CSP systems (LF, PT, and ST) under the same simulation assumptions, (ii) the integration of the electricity generation and the SWRO demand in a grid-connected annual offset configuration, and (iii) the benchmarking of the systems through discounted cash flow analysis.

The hourly meteorological data from the NSRDB Typical Meteorological Year (TMY) dataset is used to simulate hourly electricity production profiles for each technology, which are then summed to annual values. The electricity demand for SWRO is set at 160 GWh/year and is modeled as a continuous baseload; under the annual-offset assumption, annual solar production is subtracted from annual SWRO demand, while the grid is assumed to balance hourly imbalances, allowing for a fair comparison across technologies without storage. For the techno-economic analysis, a set of uniform cost and financial parameters is applied to all systems, and LCOW, NPV, and total revenue over the project life are calculated for comparative benchmarking.

2.1. System Description

Jubail, a major industrial and residential center on the Arabian Gulf, is located in the Eastern Province of Saudi Arabia, with a reported population of 474,679 inhabitants within the city limits (2022) and a total population of 505,162 inhabitants within the governorate area [23]. A population of 500,000 inhabitants, representing a mid-term planning horizon for water supply needs of a metropolitan area, shall be used for the purposes of this study, falling within the range of the reported populations for the city and governorate, and aligning with recent projections of a metropolitan area population of 700,000 inhabitants and growing [24].

Domestic water usage in Saudi Arabia is among the highest in the world. A study on water resources and sector-wise water consumption in the country states that domestic water usage per capita per day in 2009 was around 226 L/cap per day, with a strong rate of growth in municipal water demand [25].

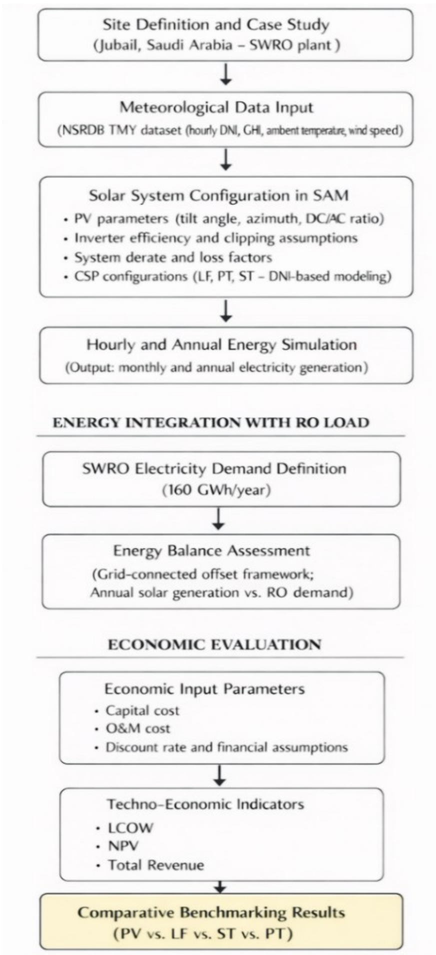

Fig. 5. Integrated methodological workflow linking SAM-based solar simulation, SWRO electricity demand integration, and techno-economic evaluation for comparative benchmarking.

A recent study on water consumption behavior of domestic consumers in Saudi Arabia states that the average water usage per capita per day for residential areas was around 300 L/cap per day, especially in major cities [26]. Accordingly, SWRO desalination is selected as the supply-side option to satisfy the expected municipal water demand under arid conditions and limited renewable freshwater resources.

Desalination system is designed to satisfy the demand of Jubail strip. The RO system was a single stage with eight vessels pressure of (SW30XHR-440i) type. About 45.625 million m^3 per year is required and this is equivalent to 5,208 m^3/h. A saline water flow rate of 14,881 m^3/h at a temperature of 25°C with 38,000 ppm feeds the RO system with a recovery rate of 35%, consistent with values commonly reported in the literature for seawater desalination applications [27].

2.2. RO System Specifications

Desalination system design is based on the adopted SWRO sizing and operating assumptions, and the main system characteristics and output results are described in Table 1.

Table 1. RO system specifications.

Parameter	Value	Parameter	Value
Saline water flow rate	14,881 m^3/h	Permeate flow rate	5,208 m^3/h
Feed pressure	57.97 bar	Energy required	3.5 kWh/m^3
Feed TDS	38,000 ppm	Number of pressure vessels	670
No. of elements	8	Feed temperature	25℃

The specific energy consumption (SEC) of SWRO plants has decreased significantly with advances in membranes, high-efficiency pumps and ERDs. A comprehensive review of more than 70 large SWRO plants by Kim et al. (2020) shows that modern plants typically operate in the range 2.5-4.0 kWh/m^3, depending on plant size, feed salinity and recovery ratio. More recent assessments report that many full-scale plants still require 3.0-4.5 kWh/m^3, especially for highly saline seawater and conservative recoveries [15]. Based on these ranges, an SEC of 3.5 kWh/ m^3 is selected as a representative value for the present case study.

Using this SEC of 3.5 kWh/m^3 and the average permeate production; the average electrical power demand of the RO plant is:

$$\text{Power} = \text{SEC} \times \text{Volume flow rate} \quad (1)$$

$$\text{Power} = 3.5 \times 5{,}208 = 18.2 \text{ MWe}$$

The corresponding annual permeate volume and annual electricity consumption are:

$$\text{Volume flow rate} = 125{,}000 \times 365 = 45.625\times10^6 \text{ m}^3/\text{year} \quad (2)$$

$$\text{Energy} = \text{SEC} \times \text{Volume flow rate} \quad (3)$$

$$\text{Energy} = 3.5 \times 45.625\times10^6 = 160 \text{ GWh/year}$$

In the subsequent SAM software simulations, this energy is treated as a continuous base-load electrical demand that must be supplied by PV, CSP under Jubail meteorological conditions under the same meteorological input dataset and evaluation assumptions described in the methodology, enabling consistent techno-economic comparison across technologies.

2.3. PV System

A PV system is primarily composed of a solar cell array, and its delivered output depends not only on the modules but also on balance-of-system components such as inverters and electrical losses, which condition the generated power [28]. PV panels convert sunlight directly into electricity [18], which makes PV a straightforward option for supplying SWRO demand because it produces electrical power without an intermediate thermal conversion step. In this study, PV operation is evaluated within the same grid-connected annual offset premise used for all technologies, ensuring consistency in the comparison basis. The PV system specifications used in this case study are tabulated in Table 2 and are set to satisfy the RO system energy consumption.

2.4. Parabolic Trough Collector

PT technology is a commercially established CSP option that generates electricity through thermal conversion. The system operates by concentrating solar radiation onto a linear receiver located along the focal line, where the absorbed heat is transferred to a heat transfer fluid (HTF) and then converted into electricity via a power block [29]. In this study, the HTF is modeled as synthetic oil (Therminol VP-1), and the PT configuration is selected to provide an electricity output scale that enables annual offset benchmarking against the SWRO demand under the same framework used for PV and the other CSP technologies. The PT system specifications are summarized in Table 3.

Table 2. PV system specifications.

System parameter	Value
Module	DNA-144-BF10-530W
System nameplate size	75,047 kW
DC to AC ratio	1.36
Rated inverter size	56,741 kW
Inverter efficiency	97.5 %
Array type	1-Axis (Tracking the sun)
Array tilt	0 degrees
Total system losses	13.4 %
Shading	no
Degradation rate	0.5%/year

Table 3. PT system specifications.

System parameter	Value
Collector type	Sky Fuel sky trough 80 mm OD receiver
Receiver name	Schott PTR80
Estimated output power	75.6 MWe
Field HTF fluid	Therminol VP-1
Designed intensity	950 W/m^2
Field aperture	363,621 m^2
Actual solar multiple	2
Collector tilt	0 deg

2.5. Linear Fresnel Receiver

LF is another CSP technology in which the receiver is fixed while solar tracking is achieved using curved or flat mirror arrays, unlike parabolic trough concentrators. This configuration can offer simpler structures, reduced wind loads, and potentially lower capital cost while maintaining scalability for power generation [30]. In the present work, LF is simulated in SAM under the same meteorological inputs and benchmarking premise used for PV and PT, and its system characteristics are reported in Table 4.

Table 4. LF system specifications.

System parameter	Value
Solar Multiple	2.3
Field aperture	877,000 m^2
Designed intensity	950 W/m^2
Solar field area	310.52 acres
Receiver model type	Evacuated tube model
Length of the collector module	89.6 m
Reflective aperture area of the collector	940.6 m^2
Estimated Power output	100.8 MWe
Thermal cycle efficiency	39.7%
Boiler pressure	7 MPa
Condenser pressure	0.166 MPa
Degradation rate	0.5%

2.6. Solar Tower

ST, also known as a central receiver system, is a CSP technology in which a heliostat field concentrates solar radiation onto a receiver located at the top of a tower, transferring thermal energy to the power generation system [31]. Two common receiver configurations are cavity and external receivers, and the principal advantages of central receiver systems include high concentration ratios and higher operating temperatures (up to 550℃), which can improve conversion performance relative to line-focus technologies under suitable operating conditions [32]. In this study, molten salt (60% $NaNO_3$ and 40% KNO_3) is used as the heat transfer fluid, and the modeled ST configuration (Table 5) is evaluated within the same annual-offset benchmarking structure used for PV, PT, and LF.

Table 5. ST system specifications.

System parameter	Value
Design gross output	65 MWe
Estimated gross to conversion factor	0.9
Cycle thermal efficiency	0.412
Estimated out power	57.78 MWe
Solar multiple	2.4
Designed intensity	950 W/m^2
Land area	2,079 acres
Boiler pressure	10 MPa
Condenser pressure	0.2 MPa
Degradation rate	0.5 %

2.7. Techno-Economic Evaluation Framework

The economic evaluation is based on the parameters listed in Table 6 (project life 25 years, real discount rate 5.5%, and water tariff 2.14 USD/m^3, among other inputs). These assumptions were applied consistently across all technologies.

Table 6. Data used for the economic evaluation of plants [33].

Parameter	Value
Project life	25 years
Interest rate	8 %
Inflation rate	2.5 %
Real discount rate	5.5 %
Sales tax (% of indirect cost basis)	5 %
Insurance (% of installed cost)	0.5 % / year
Internal rate of return (IRR)	5.7 %
Water tariff	2.14 USD/m^3

The cost comparison is based on the levelized cost of water (LCOW). The SWRO-only component is computed as:

$$LCOW_{RO} = (\text{Capital Cost} \times CRF + \text{Annual O\&M Cost}) / \text{Annual Water Production} \quad (4)$$

where CRF is the capital recovery factor. The SWRO cost input (capital and operating components) are summarized in Table 7.

Table 7. Data used for calculating the LCOW.

Parameter	Value	Ref.
Capital ($/m^3 per day)	1,917	[11]
MARR (%)	5.5	[11]
n (years)	25	[11]
CRF	0.0745	-
Operational ($/m^3)	0.16	[33]

The solar-electricity contribution to water cost is calculated using [11]:

$$LCOW_S = LCOE \times SEC \quad (5)$$

where LCOE is the levelized cost of electricity from SAM in USD/MWh, and SEC is the specific energy consumption in kWh/m^3. For the total system, the following equation is used:

$$LCOW = LCOW_{RO} + LCOW_S \quad (6)$$

3. RESULTS AND DISCUSSION

This section discusses the results of the technical and economic performance of the four solar electricity generation systems considered, namely PV, PT, LF, and ST, in providing the electrical demand of the SWRO desalination plant located in Jubail, Saudi Arabia, under a grid-connected annual offset scenario. The electrical demand of desalination plant is assumed to be constant at 160 GWh/year, while all simulations and techno-economic analysis of the systems considered were done using SAM assuming similar conditions. To make a fair comparison of the solar systems considered and isolate the effects of the technology, all solar power plant simulations were done without any form of energy storage.

3.1. Solar Resource and Simulated Monthly Energy Output

The monthly DNI values for Jubail, as used in SAM, are presented in Fig. 6. The DNI values gradually increase from winter to summer, peaking in June at approximately 250

W/m², and remaining high in August-September at around 235-245 W/m², followed by a decrease towards winter, with the lowest value in December at about 165 W/m². As DNI has a direct impact on the performance of concentrating solar power plants, the electricity generation is also expected to be high during the period of high DNI (May to October).

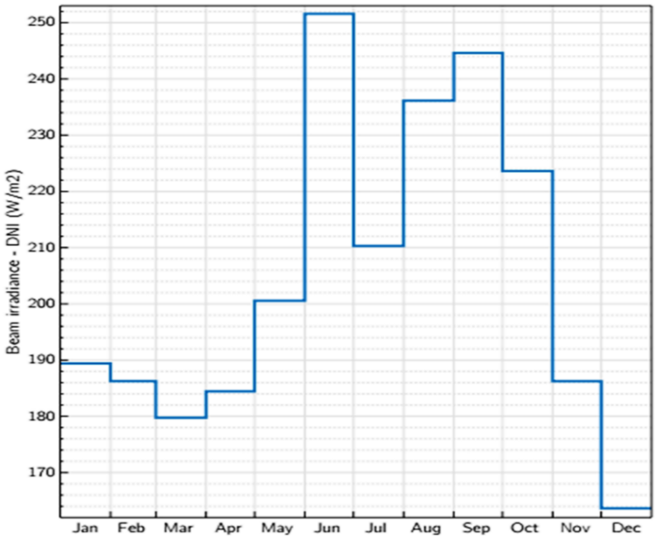

Fig. 6. Weather data for Jubail city.

A comparison of the simulated monthly electricity generation of the evaluated systems is presented in Fig. 7. According to the results, the LF system presents the highest electricity generation levels between May and October, which corresponds to the high DNI period. However, the LF system presents the greatest reduction in the winter months compared to the other systems under the same conditions.

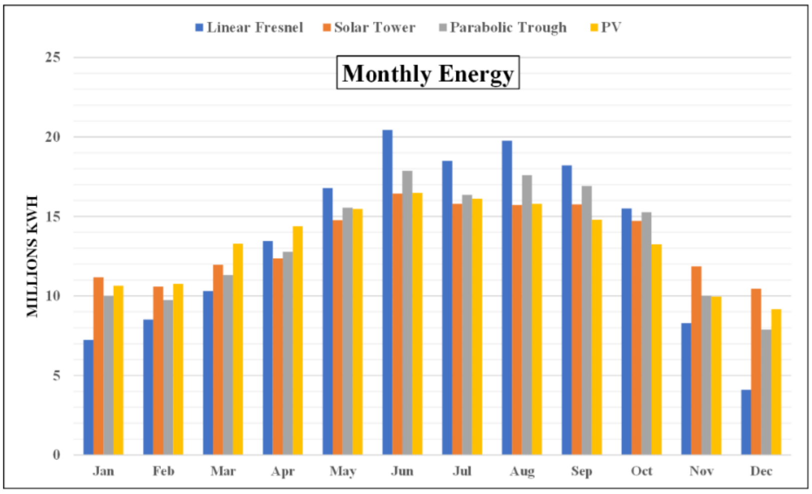

Fig. 7. Monthly energy produced from every system over a year.

Beyond energy yield, SAM provides the LCOE for each solar technology under the same financial and cost assumptions adopted in this study. The SAM-derived LCOE values are summarized in Table 8 and are subsequently used to quantify the solar-electricity contribution to the LCOW.

3.2. LCOW

Using the LCOE values in Table 8 and the LCOW formula presented in the methodology section, the total LCOW is determined for each of the solar-powered SWRO systems and compared in Fig. 8. The LCOW ranking of the four solar-powered SWRO systems is evident in the figure. The solar-powered SWRO plant has the minimum LCOW value of 0.82 USD/m^3, making it the most cost-effective solution under the assumptions made in this case study. On the other hand, the CSP-powered systems have relatively higher LCOW values of 1.44 USD/m^3 for PT, 1.52 USD/m^3 for ST, and 1.77 USD/m^3 for LF compared to the solar-powered plant with an LCOW value of 0.82 USD/m^3. The LCOW of the CSP-powered systems is relatively higher than that of the solar-powered plant, by 76% for PT, 85%. The key factor that contributes to the increased LCOW for CSP technologies is the additional solar thermal infrastructure required for CSP compared to the more straightforward electricity conversion process of PV. It is important to note that storage is not considered in this assessment; thus, the outcome is based solely on the cost competitiveness in terms of direct solar availability. The operational benefit of CSP dispatchability, when thermal storage is integrated, is not within the scope of this assessment.

Table 8. The LCOE for every solar system.

Solar technology	LCOE [USD/MWh]
PV	14.5
ST	25.5
PT	22.9
LF	30.8

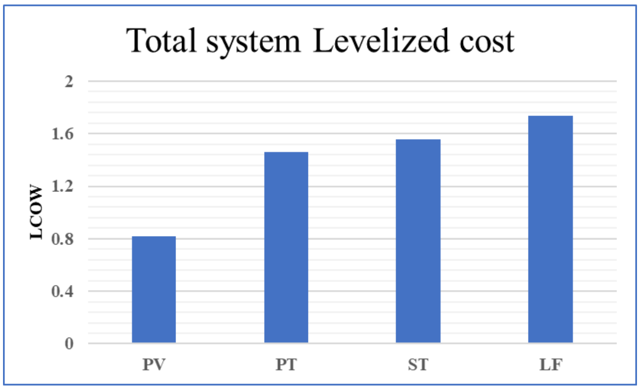

Fig. 8. Total levelized cost for every solar system.

3.3. NPV and Revenue

The NPV assessment indicates that all configurations are economically feasible under the stated assumptions, as all NPVs are positive (Fig. 9). The NPVs for PV, PT, ST, and LF are 0.96, 13.21, 17.61, and 18.95 million USD, respectively. Although PV provides the lowest LCOW, it yields the lowest NPV, demonstrating that minimum LCOW does not necessarily imply maximum profitability, because NPV depends on the magnitude and timing of lifetime cash flows rather than unit cost alone.

Fig. *10* shows the total revenue accumulation over the 25-year project life for the four system configurations: (a) PV, (b) LF, (c) ST, and (d) PT. Based on the grid-connected annual offset assumption, the electricity demand of the SWRO plant is satisfied on an annual basis; hence, the main difference in the total revenue and NPV for the different system configurations is based on the financial performance derived from the SAM simulations rather than the annual water production rates. For all system configurations, the total revenue increases with time, which shows that the annual cash flows are steady based on the operating and revenue assumptions used. It is also important to note that the scales used in the subplots are not the same, meaning that the total revenue accumulation for the different technologies has different earning potentials. Therefore, system configurations with higher total revenues have higher NPV values, regardless of their LCOW costs.

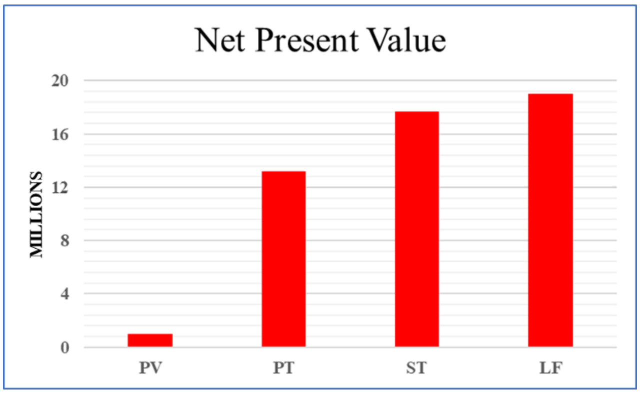

Fig. 9. The net present value for every solar system.

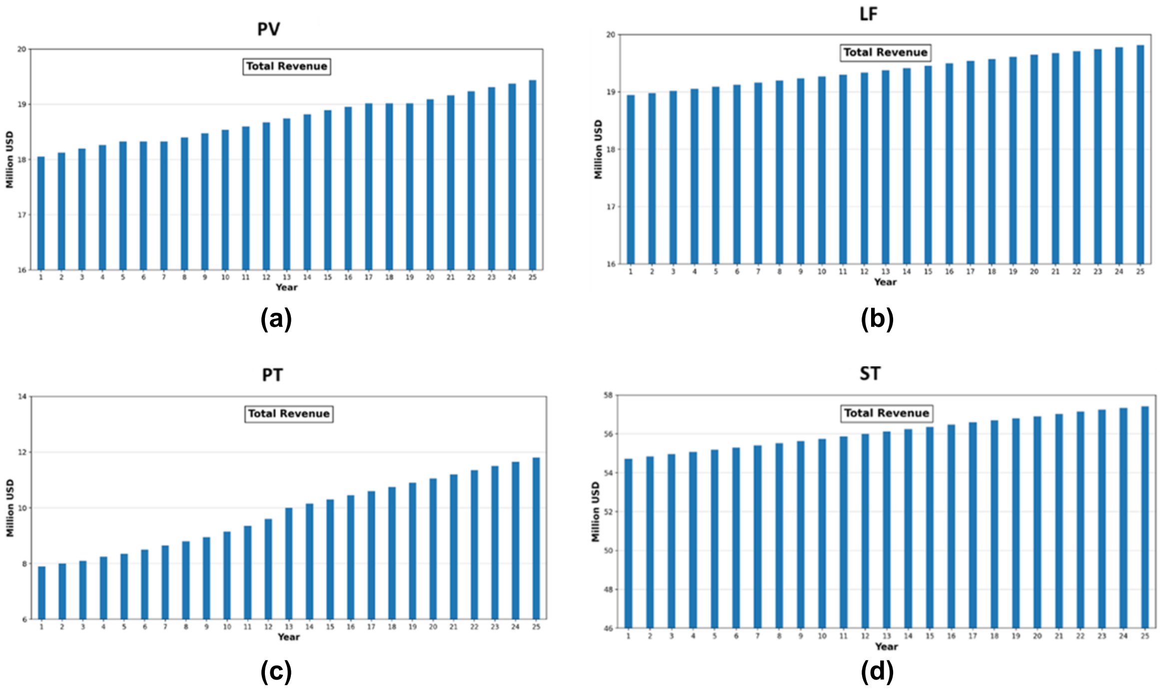

Fig. 10. Total revenue over the project lifetime: a) PV; b) LF; c) ST; and d) PT.

4. LIMITATIONS AND FUTURE WORK

The current evaluation also has a number of limitations that need to be taken into account when interpreting the findings. First, the comparison was done without considering energy storage to enable the evaluation of the basic techno-economic performance of the different solar arrangements under the same operational structure; hence, the comparison of the systems might be affected by the addition of energy storage, depending on the type and dispatch method of the storage technology. Further, the findings are location-specific, as the simulation is based on the chosen weather data for Jubail; hence, variations in the solar resource characteristics, especially DNI, might affect the monthly energy output and the techno-economic viability of CSP options. Economically, the results for the LCOW, NPV, and lifetime revenue are sensitive to the assumed capital cost, O&M cost, and economic parameters. Differences in these parameters could change the extent of the economic results and could have an impact on the technology choice for different market scenarios. In addition, the economic analysis uses simplified representations of operation compared to actual projects, where details of component degradation, down time, and other operational factors could impact the long-term results.

Future research should therefore include the development of the framework to include the modeling of storage-enabling operation and optimal dispatch, as well as sensitivity and uncertainty analysis of the key cost and economic factors. Additional locations and design optimization would also help to improve the applicability of the findings to actual hybrid solar-powered desalination projects.

5. CONCLUSIONS

A comparative study on freshwater production using a RO desalination system integrated with four different solar technologies was conducted. The comparison was carried out based on key economic indicators, namely the net present value NPV and the LCOW, for each power plant configuration. The results show that, among the investigated systems, the PV power plant represents the most economical option for supplying the electrical energy required to operate the RO desalination system. This conclusion is mainly attributed to the lower levelized cost associated with the PV system compared to the other solar technologies. It should be noted that the obtained economic values are specific to the considered configurations and operating assumptions and are expected to change when energy storage systems are incorporated into the analysis.

Acknowledgement The author gratefully acknowledges the institutional support of King Fahd University of Petroleum & Minerals, Saudi Arabia, which provided a supportive research environment for this paper. The author also acknowledges Omar Al-Mukhtar University, Libya, for its academic support and encouragement during the development of this study.

REFERENCES

[1] V. Bhakar, D. Kumar, N. Sai, K. Sangwan, S. Raghuvanshi, "Life cycle assessment of filtration systems of reverse osmosis units: a case study of a university campus," *Procedia CIRP*, vol. 40, pp. 268–273, 2016, doi: 10.1016/j.procir.2016.01.119.

[2] V. Ravinandrasana, C. Franzke, "The first emergence of unprecedented global water scarcity in the Anthropocene," *Nature Communications*, vol. 16, no. 1, p. 8281, 2025, doi: 10.1038/s41467-025-63784-6.

[3] F. Ward, "Addressing global water challenges in 2025: an integrated framework for research, policy, and resource management," *Water Resources Management*, vol. 39, no. 15, pp. 7885–7918, 2025, doi: 10.1007/s11269-025-04341-0.

[4] O. Behar, A. Khellaf, K. Mohammedi, "A review of studies on central receiver solar thermal power plants," *Renewable and Sustainable Energy Reviews*, vol. 23, pp. 12–39, 2013, doi: 10.1016/j.rser.2013.02.017.

[5] G. Ding, S. Ghosh, *Sustainable Water Management-A Strategy for Maintaining Future Water Resources*, Elsevier, 2017.

[6] J. Lundqvist, O. Unver, "Alternative pathways to food security and nutrition – water predicaments and human behavior," *Water Policy*, vol. 20, no. 5, pp. 871–884, 2018, doi: 10.2166/wp.2018.171.

[7] M. Ranjbar, H. Yousefi, M. abdoos, F. Astaraei, M. Rad, "Addressing water scarcity and energy sustainability through PV-desalination systems: a case study on the southern coast of Iran," *Energy Nexus*, vol. 18, p. 100425, 2025, doi: 10.1016/j.nexus.2025.100425.

[8] M. Saleem, M. Ali, "Sustainable energy measures in Saudi Arabia based on renewable energy sources: present actions and future plans," 4th International Conference on Energy, Environment and Sustainable, 2016.

[9] Z. Al Suleimani and V. Nair, "Desalination by solar-powered reverse osmosis in a remote area of the Sultanate of Oman," *Applied Energy*, vol. 65, no. 1, pp. 367–380, 2000, doi: 10.1016/S0306-2619(99)00100-2.

[10] M. Methnani, "Influence of fuel costs on seawater desalination options," *Desalination*, vol. 205, no. 1, pp. 332–339, 2007, doi: 10.1016/j.desal.2006.02.058.

[11] U. Caldera, C. Breyer, "Learning curve for seawater reverse osmosis desalination plants: capital cost trend of the past, present, and future," *Water Resources Research*, vol. 53, no. 12, pp. 10523–10538, 2017, doi: 10.1002/2017WR021402.

[12] A. Alkaisi, R. Mossad, A. Sharifian-Barforoush, "A review of the water desalination systems integrated with renewable energy," *Energy Procedia*, vol. 110, pp. 268–274, 2017, doi: 10.1016/j.egypro.2017.03.138.

[13] G. Zhang, X. Wang, "Seawater desalination system driven by sustainable energy: a comprehensive review," *Energies*, vol. 17, p. 57062024, doi: 10.3390/en17225706.

[14] M. Baseer, A. Alqahtani, S. Rehman, "Techno-economic design and evaluation of hybrid energy systems for residential communities: case study of Jubail industrial city," *Journal of Cleaner Production*, vol. 237, p. 117806, 2019, doi: 10.1016/j.jclepro.2019.117806.

[15] J. Kim, K. Park, D. Yang, S. Hong, "A comprehensive review of energy consumption of seawater reverse osmosis desalination plants," *Applied Energy*, vol. 254, p. 113652, 2019, doi: 10.1016/j.apenergy.2019.113652.

[16] S. Chowdhury, M. Al-Zahrani, "Characterizing water resources and trends of sector wise water consumptions in Saudi Arabia," *Journal of King Saud University - Engineering Sciences*, vol. 27, no. 1, pp. 68–82, 2015, doi: 10.1016/j.jksues.2013.02.002.

[17] A. Almulhim, I. Abubakar, "A segmentation approach to understanding water consumption behavioral patterns among households in Saudi Arabia for a sustainable future," *Resources, Environment and Sustainability*, vol. 15, p. 100144, 2024, doi: 10.1016/j.resenv.2023.100144.

[18] M. Grätzel, "Photovoltaic and photoelectrochemical conversion of solar energy," *Philosophical Transactions Series A, Mathematical, Physical, and Engineering Sciences*, vol. 365, no. 1853, pp. 993–1005, Feb. 2007, doi: 10.1098/rsta.2006.1963.

[19] N. Ghaffour, T. Missimer, G. Amy, "Combined desalination, water reuse, and aquifer storage and recovery to meet water supply demands in the GCC/MENA region," *Desalination and Water Treatment*, vol. 51, no. 1, pp. 38–43, 2013, doi: 10.1080/19443994.2012.700034.

[20] T. Ajiwiguna, G. Lee, B. Lim, S. Cho, C. Park, "Optimization of battery-less PV-RO system with seasonal water storage tank," *Desalination*, vol. 503, p. 114934, 2021, doi: 10.1016/j.desal.2021.114934.

[21] S. Goutte, K. Klotzner, H. Le, and H. Mettenheim, "Forecasting photovoltaic production with neural networks and weather features," *Energy Economics*, vol. 139, p. 107884, 2024, doi: 10.1016/j.eneco.2024.107884.

[22] R. Madhuri, Z. Said, I. Ihsanullah, R. Sathyamurthy, "Solar energy-driven desalination: a renewable solution for climate change mitigation and advancing sustainable development goals," *Desalination*, vol. 602, p. 118575, 2025, doi: 10.1016/j.desal.2025.118575.

[23] R. Engelman, "People in the Balance," Population Action International, 2000, https://www.populationaction.org

[24] M. Baig, A. Al Kutbi, "Design features of a 20 migd SWRO desalination plant, Al Jubail, Saudi

Arabia," *Desalination*, vol. 118, no. 1, pp. 5–12, 1998, doi: 10.1016/S0011-9164(98)00068-X.
[25] A. Vigotti, "Workshop on Renewable Energy and Water," IEA Working Party on Renewable Energy Technologies, 2009.
[26] M. Mohammed, S. Boghandora, A. Belkhair, "Techno-economic analysis of wind and geothermal energy for reverse osmosis desalination : a case study of Tripoli," *Journal of Power and Energy Engineering,* vol. 13, no. 11, pp. 86–109, 2025, doi: 10.4236/jpee.2025.1311006.
[27] A. Nada, M. Sharaan, M. Elshemy, M. Fujii, M. Ibrahim, "Scaling and corrosion dynamics for full-scale SWRO desalination plants in Egypt: challenges and mitigation strategies," *International Journal of Environmental Science and Development*, vol. 16, no. 4, pp. 278–285, 2025, doi: 10.18178/ijesd.2025.16.4.1535.
[28] A. Al-Ezzi, M. Ansari, "Photovoltaic solar cells: a review," *Applied System Innovation,* vol. 5, no. 4, p. 67, 2022, doi: 10.3390/asi5040067.
[29] A. Biswas *et al.*, "Water scarcity: A global hindrance to sustainable development and agricultural production – a critical review of the impacts and adaptation strategies," *Cambridge Prisms: Water*, vol. 3, p. e4, 2025, doi: doi: 10.1017/wat.2024.16.
[30] M. Ahmadi *et al.*, "Solar power technology for electricity generation: A critical review," *Energy Scince Engineering*, vol. 6, no. 5, pp. 340–361, 2018, doi: 10.1002/ese3.239.
[31] C. Wang, L. Wang, L. Dong, H. Shon, J. Kim, "Specific energy consumption of seawater reverse osmosis desalination plants using machine learning," *Desalination*, vol. 602, p. 118654, 2025, doi: 10.1016/j.desal.2025.118654.
[32] O. Mohammed, Y. Amirat, M. Benbouzid, "Economical evaluation and optimal energy management of a stand-alone hybrid energy system handling in genetic algorithm strategies," *Electronics*, vol. 7, no. 10, p. 233, 2018, doi: 10.3390/electronics7100233.
[33] M. Saleem, M. Bin-Saleem, M. Bin-Saleem, M. Ali, E. Mahrous, "Energy transition in Saudi Arabia: harnessing solar solutions for a sustainable future renewable energy blend while navigating challenges and capitalizing on opportunities," *Renewable Energy and Sustainable Development*, vol. 11, no. 2, 2025, doi: 10.21622/RESD.2025.11.2.1319.